Progress In Electromagnetics Research M, Vol. 104, 213–222, 2021

Design and Analysis of Polarization-Insensitive Broadband Microwave Absorber for Perfect Absorption

Sudha Malik[1, *], Mondeep Saikia[1], Aditi Sharma[1], Gaganpreet Singh[2], Janakrajan Ramkumar[2], Puneet K. Mishra[3], and Kumar V. Srivastava[1]

Abstract—A simple design configuration of a broadband polarization-insensitive double-layered microwave absorber is presented here. The proposed absorber is designed using indium tin oxide (ITO) based on thin resistive film. The novelty of structure is to achieve large absorption bandwidth with more than 99% absorption. The proposed structure is modeled for 20 dB absorption bandwidth at normal incidence from 6.3 GHz to 14.2 GHz spanning over C-band, X-band, and Ku-band. Under oblique incidence the proposed structure is stable up to 60° for TE polarization and 45° for TM polarization. To understand the operating principle of absorption of the proposed structure, an equivalent circuit is derived, and surface current distribution is also studied. A fabricated sample is measured, which validates our simulation.

1. INTRODUCTION

Microwave absorbers have many applications in various domains like stealth technology, radar cross-section reduction, EM compatibility, solar absorber, etc. [1–4]. The first microwave absorber Salisbury screen was introduced by Winfield Salisbury. In the Salisbury screen, a resistive sheet of 377 Ω is placed at a distance of quarter wavelength from the ground plane [5, 6]. When a plane wave with the appropriate wavelength is incident normally upon the resistive sheet, it is dissipated as heat due to ohmic loss. At a particular frequency, where the spacing between the resistive sheet and the ground plane is $\lambda/4$, the short circuit becomes an open circuit. If the resistive sheet has an impedance of 377 Ω, then the input impedance of the screen will be perfectly matched to the free space impedance resulting in perfect absorption at that frequency, but it has the disadvantage of narrowband absorption. Jaumann absorber is an extended version of the Salisbury screen, which consists of two or more resistive sheets, and resistive sheets are separated by $\lambda/4$ distance [7]. The disadvantage of Jaumann is the increased overall thickness. Pyramidal absorbers are most extensively used to achieve a low reflection coefficient (40 dB) [8]. However, these absorbers are heavy and fragile to handle, thus find limited applications. For decreasing the thickness of conventional absorbers, metamaterial absorbers are designed. In [9–11], triple band absorbers are designed using FR-4 with different thicknesses, which gives near unity absorption. However, these absorbers do not give broadband absorption.

To reduce the thickness and increase the bandwidth, frequency selective surface (FSS) based circuit analog (CA) absorbers are designed [12–23]. The circuit analog absorber consists of resistive as well as reactive components which are printed on a dielectric substrate and terminated by a metal ground plane. FSS based circuit analog absorber is usually designed for 10 dB of absorption over a frequency band. But here, 20 dB return loss is targeted as it ensures more than 99% absorption in a wide frequency range.

Received 27 June 2021, Accepted 13 September 2021, Scheduled 22 September 2021

* Corresponding author: Sudha Malik (sudhamalik1@gmail.com).

[1] Department of Electrical Engineering, Indian Institute of Technology Kanpur (IITK), 208016, India. [2] Department of Mechanical Engineering, Indian Institute of Technology Kanpur (IITK), 208016, India. [3] U R Rao Satellite Centre, ISRO Satellite Integration and Testing Establishment (ISITE), ISRO 560037, India.

The CA absorber in [12] has a fractional bandwidth of 83.01% with 10 dB of absorption bandwidth. In [13], a single layer absorber has fractional bandwidth of 70.8% with an absorption bandwidth of 10 dB. In [22], an absorber with 10 dB of absorption bandwidth has a 126.8% of fractional bandwidth. A single layer transparent absorber [23] with 88.52% fractional bandwidth has achieved 10 dB absorption bandwidth in a wide range. A combination of the Dallenbach layer and Salisbury screen in [24] has a fractional bandwidth of 70.4% for 20 dB of absorption. However, none of these structures show a broad frequency range with angular stability.

In this work, an FSS based polarization-insensitive broadband absorber has been presented, which has 20 dB absorption bandwidth for C-band, X-band, and Ku-band. The novelty of the proposed structure is showing broad absorption bandwidth from 5.59 GHz to 15.57 GHz with 95.32% of fractional bandwidth. The double-layer structure consists of ITO-based resistive film on a PET substrate. Foam is used as a spacer between top & middle layers and middle & bottom layers. Copper is used in the background. The proposed absorber is fabricated with a laser machining technique.

2. DESIGN OF STRUCTURE AND DISCUSSION OF SIMULATED RESULTS

The unit cell of the polarization-insensitive broadband absorber, which is designed to achieve 20 dB absorption bandwidth is shown in Fig. 1. The top and middle layers are composed of an ITO coated PET ($\epsilon_r = 3.2$ $\tan\delta = 0.003$) sheet of a thickness (t_p) 0.127 mm. The foam spacer of a thickness (h_1) of 4 mm separates top and middle layers, with a thickness of (h_2) 6 mm separating middle and bottom layers. The bottom layer is continuous copper with the conductivity of 5.8×10^7 S/m. The top layer consists of resistive patterns of a cross dipole and the middle layer of the modified Minkowsky loop. The surface resistance of resistive film on the top and middle layers is (R_s) 35 Ω/sq. The optimized parameters are as follows: $p = 7.3$ mm, $L = 4.5$ mm, $W = 1.4$ mm, $L_c = 2.5$ mm, $g = 0.25$ mm, $g_1 = 0.5$ mm, $W_1 = 0.7$ mm, $S = 0.25$ mm.

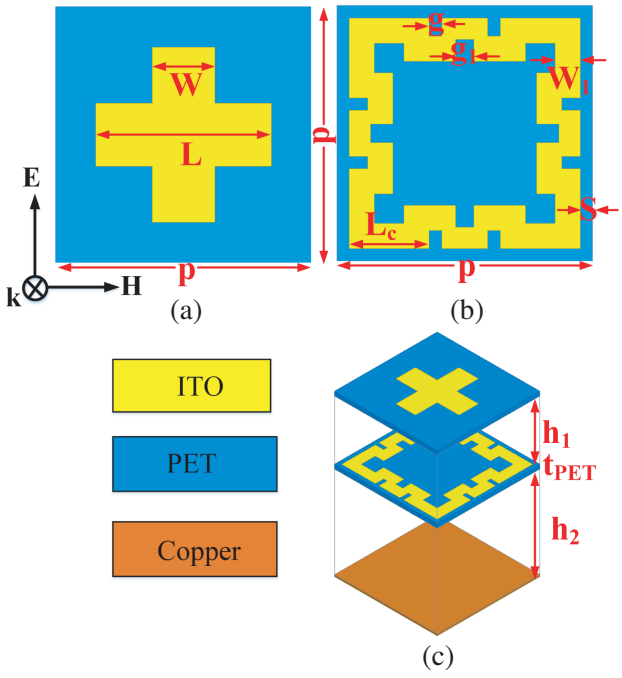

Figure 1. (a) Schematic of top layer of the proposed structure, (b) schematic of middle layer of proposed structure and (c) perspective view.

Full wave simulation of the proposed structure is performed in ANSYS HFSS software utilizing periodic boundary conditions. The reflection coefficient is illustrated in Fig. 2(a), which is observed to be less than −20 dB in 5.59–15.77 GHz, thus covering the C-, X-, and Ku-bands. The ground

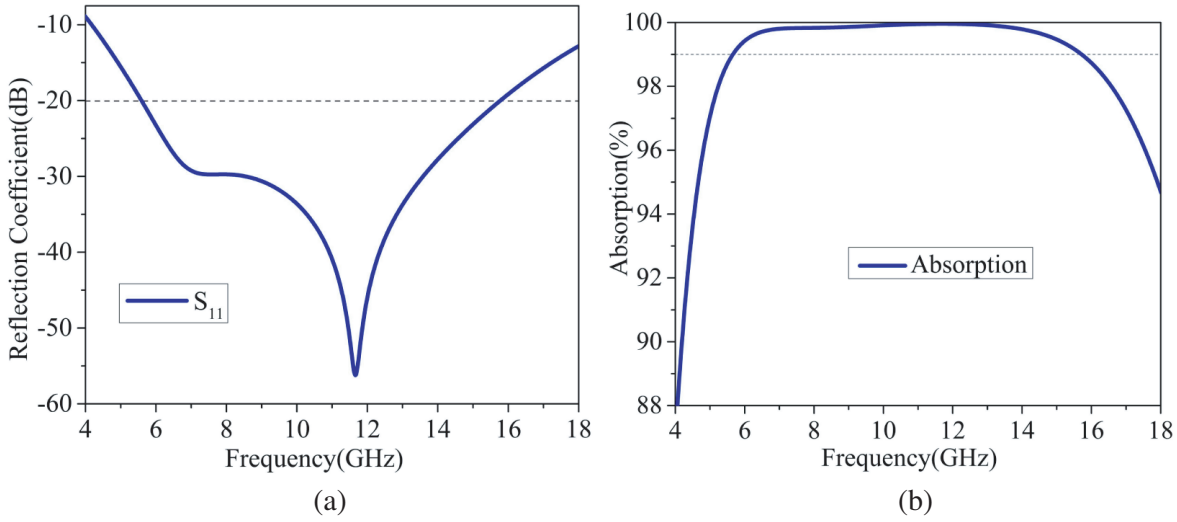

Figure 2. Simulated reflection coefficient and absorptivity under normal incidence.

plane is backed with continuous copper, which makes the transmission zero. At frequency 7.11 GHz and 11.66 GHz, two resonance dips are observed with reflection coefficients −29.45 dB and −56.21 dB, respectively. As illustrated in Fig. 2(b), the proposed design exhibits 99% absorptivity calculated by $(A = 1 - |S_{11}|^2 - |S_{21}|^2)$ in frequency range from 5.59 GHz to 15.77 GHz and thus obtains the fractional bandwidth of 95.32% with respect to the center frequency.

The designed absorber has also been investigated for different polarization angles, considering normal incidence. Fig. 3 shows the response of the absorber design for different polarization angles. As the structure is symmetrical in nature, the simulated reflection coefficient remains the same for different polarization angles, thus making the design polarization insensitive.

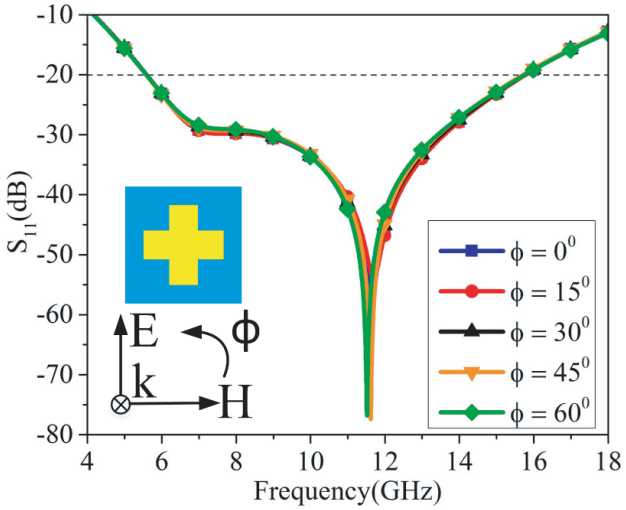

Figure 3. Simulated response of the proposed structure for different angles of polarization under normal incidence.

The performance of the proposed double-layer 20 dB broadband absorber is examined for different oblique incidence angles. Figs. 4(a) and (b) show the simulated reflection coefficient for different incidence angles for transverse electric (TE) and transverse magnetic (TM) polarized waves, respectively. For TE polarization, the response of reflection coefficient maintains the 20 dB absorption up to 60°, but

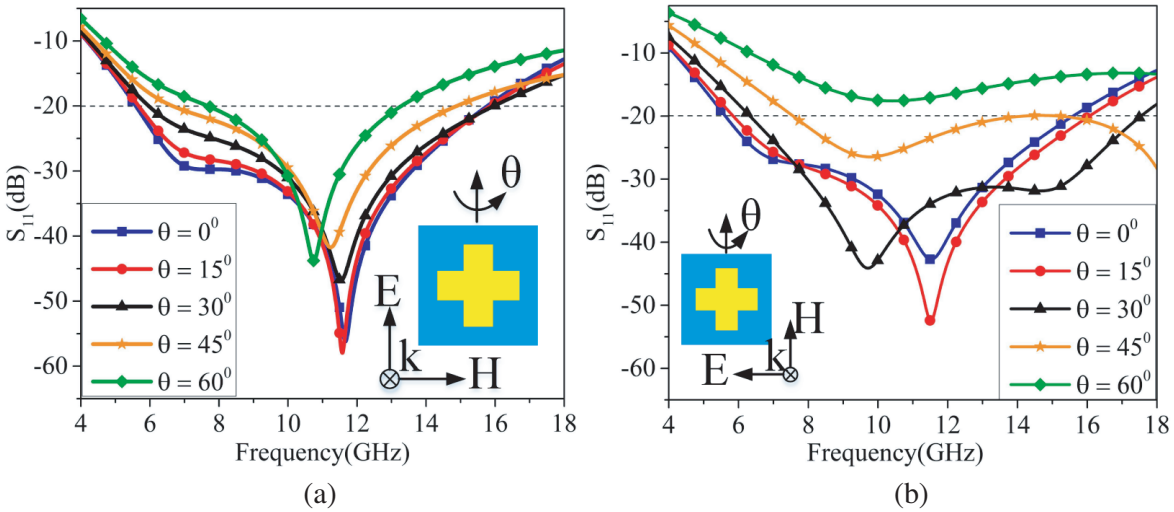

Figure 4. Reflection coefficients of the proposed absorber for different oblique incidence angle. (a) Transverse Electric polarization and (b) transverse Magnetic polarization.

bandwidth becomes narrower, whereas in the case of TM polarization response shifts slowly towards the higher frequency band.

3. MECHANISM OF ABSORPTION

The model of an equivalent circuit for the proposed structure has been developed to analyze the operating principle of the absorber, which is illustrated in Fig. 5(a). The top and middle layers are modeled as a series combination of resistor, inductor, & capacitor (RLC) circuits. The PET substrate and foam spacer are modeled as segments of transmission lines. To validate the model of an equivalent circuit of the proposed structure, the values of lumped capacitance, inductance, and resistance of the circuit model are found as: $C_1 = 13.75\,\text{fF}$, $L_1 = 1\,\text{nH}$, $R_1 = 630\,\Omega$, $C_2 = 153\,\text{fF}$, $L_2 = 1\,\text{nH}$, and

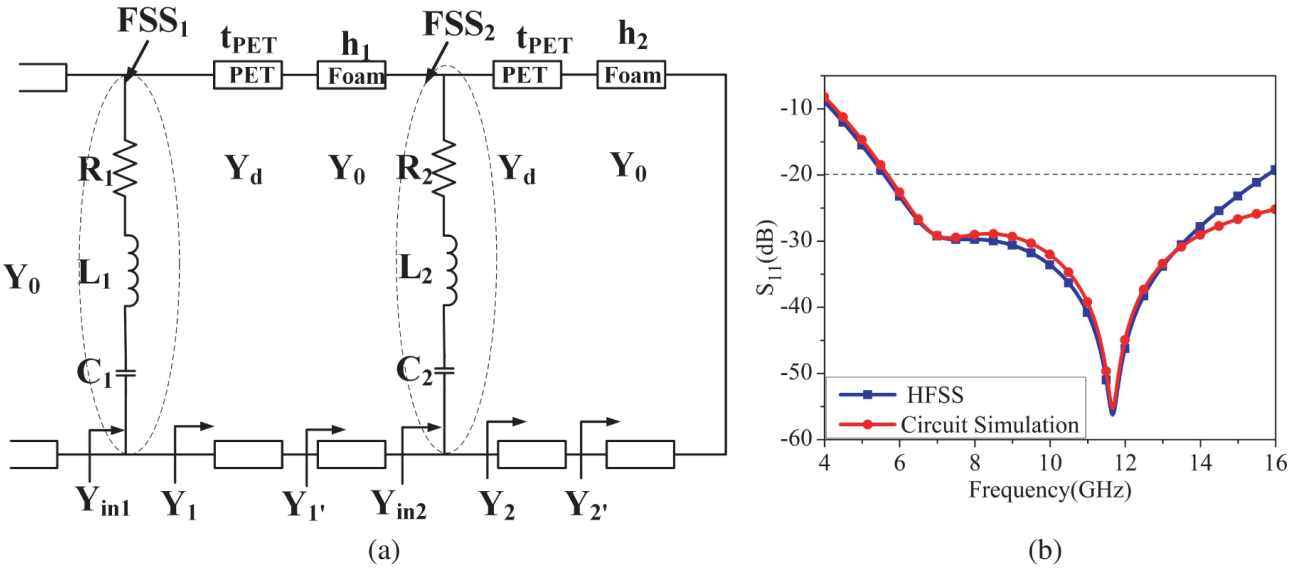

Figure 5. (a) Model of Equivalent circuit and (b) comparison of simulated response of reflection coefficient obtained by equivalent circuit model and HFSS simulation.

$R_2 = 249\,\Omega$. Fig. 5(b) displays the simulated reflection coefficient plots realized using the full wave analysis (HFSS simulations) and the circuit analysis (using the equivalent circuit model). The following equations have been derived to understand the mechanism of the proposed 20 dB absorber.

$$Y_{2'} = -jY_0 \cot \beta_0 h_2 \tag{1}$$

$Y_{2'}$ is the admittance of the ground plane looking towards the foam, Y_0 the admittance of foam, and h_2 the thickness of foam between the middle and the bottom layer.

$$Y_2 = Y_d \frac{Y_{2'} + jY_d \tan \beta_{PET} t_{PET}}{Y_d + jY_{2'} \tan \beta_{PET} t_{PET}} \tag{2}$$

Y_2 is the admittance of PET substrate, whereas t_{PET} is the thickness of PET substrate, and Y_d is the admittance of dielectric.

$$Y_{FSS2} = \frac{1}{R_2 + j\omega L_2 + \frac{1}{j\omega C_2}} \tag{3}$$

Y_{FSS2} is the admittance of the middle FSS layer, whereas R_2, L_2, and C_2 are the resistance, inductance, and capacitance of the middle FSS layer, respectively.

$$Y_{in2} = Y_{FSS2} + Y_2 \tag{4}$$

Y_{in2} is the total admittance of the middle layer. From Fig. 6(b), it is evident that B_2 and B_{FSS2} are opposite in sign, thus cancel B_{in2}, which is close to zero. From Fig. 6(a), G_2 is close to zero. Thus G_{FSS2} mainly contributes to G_{in2} and is close to $1/377\,\Omega$.

$$Y_{1'} = Y_0 \frac{Y_{in2} + jY_0 \tan \beta_0 h_1}{Y_0 + jY_{in2} \tan \beta_0 h_1} \tag{5}$$

$Y_{1'}$ is the admittance looking from PET substrate, Y_0 the admittance of foam substrate, and h_1 the thickness of foam between the top and the middle layer.

$$Y_1 = Y_d \frac{Y_{1'} + jY_d \tan \beta_{PET} t_{PET}}{Y_d + jY_{1'} \tan \beta_{PET} t_{PET}} \tag{6}$$

Y_1 is the admittance of PET substrate, whereas t_{PET} is the thickness of PET substrate, and Y_d is the admittance of dielectric.

$$Y_{FSS1} = \frac{1}{R_1 + j\omega L_1 + \frac{1}{j\omega C_1}} \tag{7}$$

Y_{FSS1} is the admittance of the top FSS layer, whereas R_1, L_1, and C_1 are the resistance, inductance, and capacitance of the top FSS layer, respectively.

$$Y_{in1} = Y_{FSS1} + Y_1 \tag{8}$$

Y_{in} is the total admittance. From Fig. 6(b), B_1 & B_{FSS1} are opposite in sign canceling each other. Thus B_{in1} vanishes in the design frequency range. From Fig. 6(a), the addition of G_{FSS1} to G_1 brings G_{in1} approximately $1/377\,\Omega$, thus achieving a near-perfect match from 5.59 GHz to 14.57 GHz.

To delve deep into the absorption mechanism of the proposed absorber, the surface current distributions of all the layers are examined at two different frequencies, i.e., 7.11 GHz and 11.66 GHz, and are plotted in Fig. 7. It is observed from Fig. 7(a) that, at 7.11 GHz, the surface current is weak at the edges but strong at the middle portion of the absorber structure. Also, it can be seen from Figs. 7(a) and 7(c) that the surface current distribution of the top layer is anti-parallel with that of the bottom layer. Hence, a magnetic resonance between the top and bottom layers occurs with a resonant frequency of 7.11 GHz. Similarly, from Figs. 7(e) and 7(f), it is observed that the currents of the middle and bottom layers also flow in the opposite direction. So, another magnetic dipole between the middle and bottom layers is formed with a resonant frequency of 11.66 GHz. On the other hand, the top resistive layer is mainly excited by the incident electric field, thus producing an electric excitation. So, it can be said that to achieve the perfect absorption, both the electric and magnetic resonances are responsible.

For a better understanding of the working of the proposed absorber, variation of different parameters is also investigated. The simulated reflection coefficient with the variation of sheet resistance

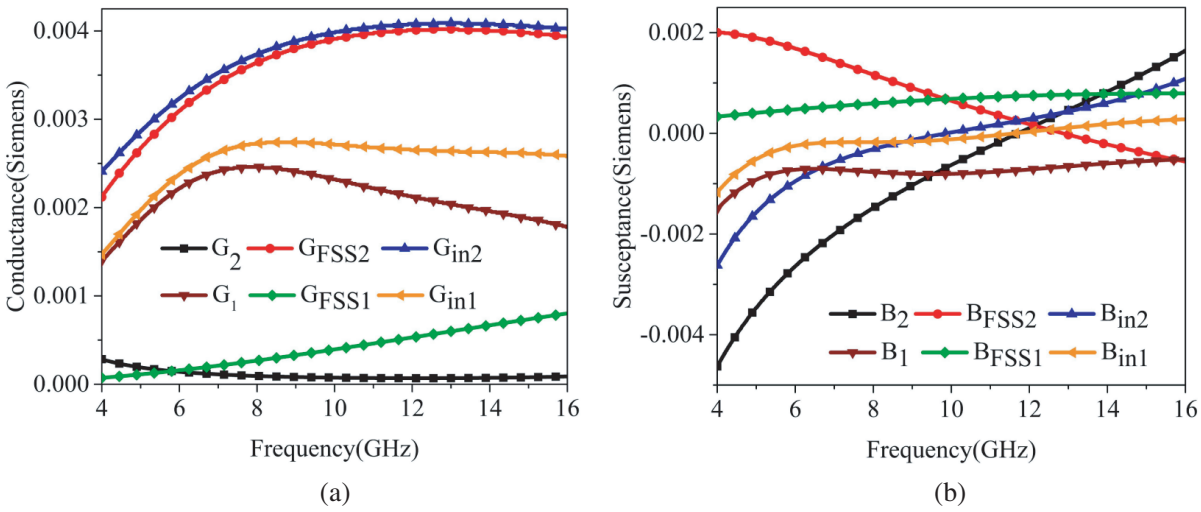

Figure 6. (a) Simulated response of conductance obtained by equivalent circuit model and (b) simulated response of susceptance obtained by equivalent circuit model.

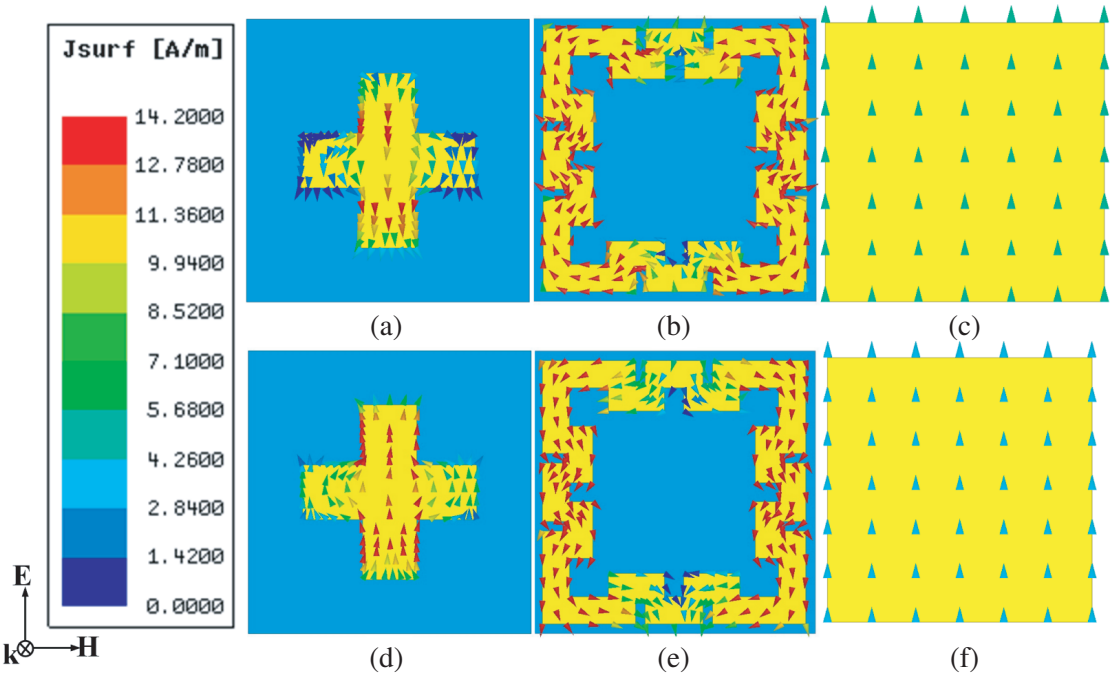

Figure 7. Surface current distribution of proposed absorber at two different frequencies. (a) 7.11 GHz, top layer, (b) 7.11 GHz, middle layer (c) 7.11 GHz, bottom layer, (d) 11.66 GHz, top layer (e) 11.66 GHz, middle layer and (f) 11.66 GHz, bottom layer.

of the top and middle layers is illustrated in Fig. 8(a). The proposed absorber maintains broadband absorption at different sheet resistances but does not provide the 20 dB of absorption bandwidth. When both layers' sheet resistances are varied from 50 Ω/sq to 100 Ω/sq, the frequency is shifted to a higher band and gives 10 dB of absorption bandwidth. Thus 35 Ω/sq seems optimum to achieve 20 dB of absorption bandwidth. The proposed structure is also studied for variation of the foam thickness. From Fig. 8(b) it is noted that, as the thickness of foam h_1 (between the top and middle layer) is increased from 4 mm to 10 mm, the absorption spectrum becomes narrow and does not maintain 20 dB of absorption

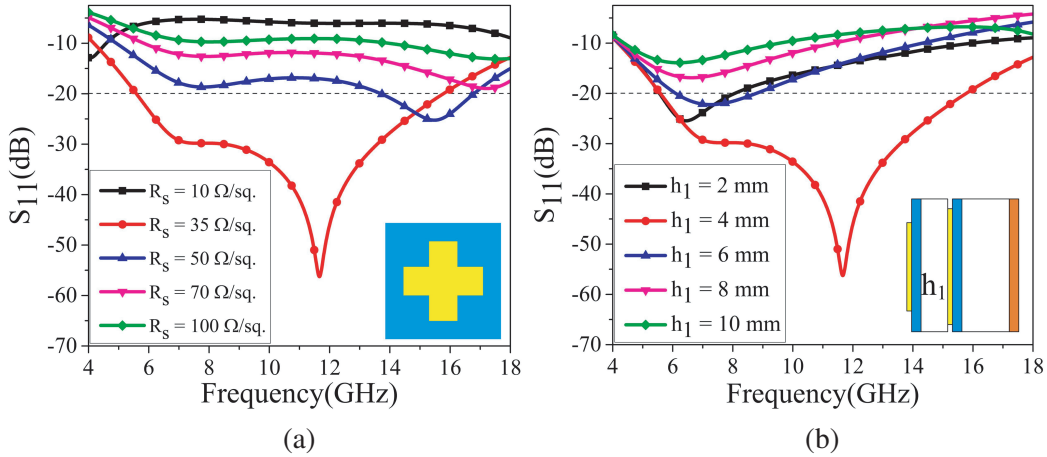

Figure 8. Simulated response of proposed absorber under normal incidence with variation of (a) sheet resistance and (b) foam spacer thickness h_1.

bandwidth.

The broad absorption bandwidth has been achieved here by introducing a double-layered configuration. The behaviors of the top and middle layers are analyzed by simulating the two layers separately, which is demonstrated in Fig. 9. Initially, in the absence of middle layer simulation has been done for the top layer only, which does not give desired results. But the middle layer gives -10 dB of reflection coefficient from the frequency range of 4.47 GHz to 15.31 GHz in the absence of the top layer. The combination of top and middle layers gives 20 dB of absorption bandwidth.

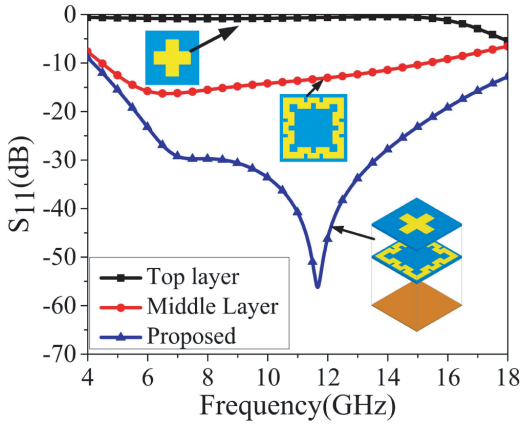

Figure 9. Simulated response of proposed absorber under normal incidence for individual top layer, middle layer and proposed absorber.

4. EXPERIMENTAL VERIFICATION

The proposed structure is also experimentally verified. The fabrication is done by using laser machining technique with KrF Excimer Laser (Coherent Variolas Complex Pro 205F). The structure with a size of 30 cm $\times$ 40 cm is fabricated, which is shown in Figs. 10(a) to 10(d). The top and middle layers are fabricated on an ITO coated PET sheet with a surface resistance of 35 Ω/sq. An ECCOSTOCK foam ($\epsilon_r = 1.03$ $\tan\delta = 0.003$) of thickness 6 mm is used as a spacer between the bottom and middle layers, and 4 mm thick foam is used between the top and middle layers. The proposed structure is measured by the free space measurement technique in an anechoic chamber. The measurement setup is shown in

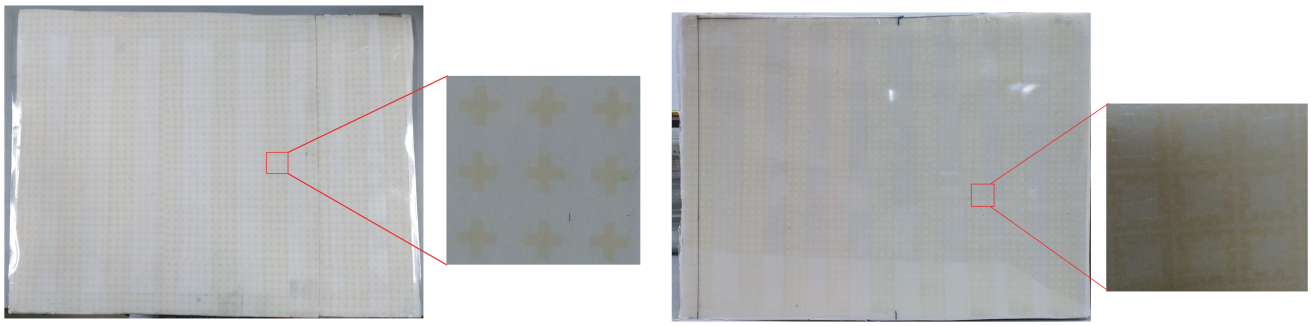

(a) (b) (c) (d)

Figure 10. Fabricated sample. (a) Top layer, (b) zoom view of top layer, (c) middle layer and (d) zoom view of middle layer.

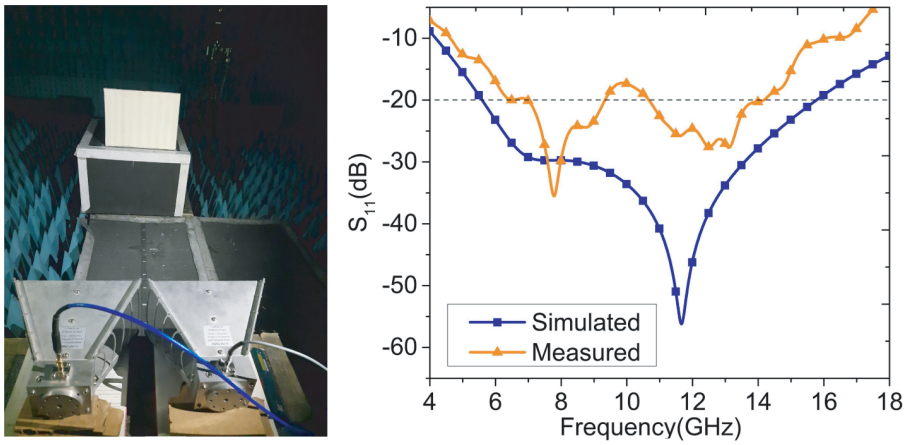

(a) (b)

Figure 11. (a) Measurement setup in an anechoic chamber and (b) simulated and measured reflection coefficients of the proposed structure under normal incidence.

Fig. 11(a), which consists of two broadband horn antennas. The sample is measured and normalized with respect to a metal plate of the same size. To enhance the measurement accuracy and lessen the background noise due to multipath propagation time gating is used. Under normal incidence, the comparison of the simulated and measured reflection coefficients is plotted in Fig. 11(b). The measured reflection coefficient is below -20 dB from the range of 6.3 GHz to 14.2 GHz.

Table 1. Comparison with other broadband absorber.

Reference	Absorption Band (GHz)	Periodicity (f_L)	Fractional BW %	Simulated Return Loss
[12]	6.06–14.66	$0.26\lambda_L$	83.01	10
[13]	8.3–17.4	$0.415\lambda_L$	70.8	10
[22]	2–9	$0.162\lambda_L$	126.8	10
[23]	8–20.7	$0.269\lambda_L$	88.52	10
[24]	5.8–12.1	Not Available	70.4	20
This Work	**5.59–15.77**	**$0.146\lambda_L$**	**95.32**	**20**

5. CONCLUSION

A design of an FSS based double-layered polarization-insensitive broadband absorber has been presented, which comprises patterned ITO resistive film coated on a PET sheet, separated by a foam spacer. The structure exhibits 20 dB absorption bandwidth, i.e., 99% absorptivity from 6.3 GHz to 14.2 GHz with a relative bandwidth of 77.07%. To validate and analyze the proposed absorber design, its equivalent circuit model is developed. As the unit cell of the structure has four-fold symmetry, the absorber design is polarization insensitive. The designed absorber is stable up to 60° and 45° for TE and TM incidences, respectively. Compared to previously reported absorbers, the absorption bandwidth of the proposed absorber increases, and periodicity is significantly improved, as observed in Table 1. The microwave absorber proposed in this paper can be used in various ground and space applications.

ACKNOWLEDGMENT

This work is funded by ISRO-IITK Space Technology Cell.

REFERENCES

1. Knott, E. F., J. F. Shaeffer, and M. T. Tuley, *Radar Cross Section*, 2nd Edition, SciTech, Raleigh, NC, USA, 2004.
2. Fallahi, A., A. Yahaghi, H. Benedickter, H. Abiri, M. Shahabadi, and C. Hafner, "Thin wideband radar absorbers," *IEEE Transactions on Antennas and Propagation*, Vol. 58, No. 12, 4051–4058, 2010.
3. Bahret, W. F., "The beginnings of stealth technology," *IEEE Transactions on Aerospace Electronic System*, Vol. 29, No. 4, 1377–1385, 1993.
4. Ono, N., Y. Hayashi, A. Kisuki, and Y. Ikeda, "Anechoic chamber and wave absorber," US Patent EP0660123 A2, 1995.
5. Fante, R. L. and M. T. McCormack, "Reflection properties of the Salisbury screen," *IEEE Transactions on Antennas and Propagation*, Vol. 36, No. 10, 1443–1454, 1988.
6. Salisbury, W. W., "Absorbent body for electromagnetic waves," US Patent 2599944, 1952.
7. Du Toit, L. J, "The design of Jauman absorbers," *IEEE Antennas and Propagation Magazine*, Vol. 36, No. 6, 17–25, 1994.
8. Emerson, W., "Electromagnetic wave absorbers and anechoic chambers through the years," *IEEE Transactions on Antennas and Propagation*, Vol. 21, No. 4, 484–490, 1973.
9. Sreenath, R., N. Mishra, and R. K. Chaudhary, "Design and analysis of an ultrathin triple-band polarization independent metamaterial absorber," *AEU — International Journal of Electronics and Communications*, Vol. 82, 508–515, Elsevier, 2017.
10. Mishra, N., D. K. Choudhary, R. Chowdhury, K. Kumari, and R. K. Chaudhary, "An investigation on compact ultra-thin triple band polarization independent metamaterial absorber for microwave frequency applications," *IEEE Access*, Vol. 5, 4370–4376, 2017.
11. Kumari, K., N. Mishra, and R. K. Chaudhary, "Wide-angle polarization independent triple band absorber based on metamaterial structure for microwave frequency applications," *Progress In Electromagnetics Research C*, Vol. 76, 119–127, 2017.
12. Sheokand, H., S. Ghosh, G. Singh, M. Saikia, K. V. Srivastava, J. Ramkumar, and S. A. Ramakrishna, "Transparent broadband metamaterial absorber based on resistive films," *Journal of Applied Physics*, Vol. 122, No. 10, 105105, 2017.
13. Zhang, C., Q. Cheng, J. Yang, and T. J. Cui, "Broadband metamaterial for optical transparency and microwave absorption," *Applied Physics Letters*, Vol. 110, No. 14, 143511, 2017.
14. Chen, J., Z. Hu, G. Wang, X. Huang, S. Wang, X. Hu, and M. Liu, "High impedance surface-based broadband absorbers with interference theory," *IEEE Transactions on Antennas and Propagation*, Vol. 63, No. 10, 4367–4374, 2015.

15. Tayde, Y., M. Saikia, and K. V. Srivastava, "Polarization-insensitive broadband multilayered absorber using screen printed patterns of resistive ink," *IEEE Antennas Wireless Propagation Letters*, Vol. 17, No. 12, 2489–2493, 2018.
16. Zhang, L., Y. Shi, J. X. Yang, X. Zhang, and L. Li, "Broadband transparent absorber based on indium tin oxide-polyethylene terephthalate film," *IEEE Access*, Vol. 7, 137848–137855, 2019.
17. Yao, Z., S. Xiao, Z. Jiang, L. Yan, and B. Wang, "On the design of ultrawideband circuit analog absorber based on quasi-single-layer FSS," *IEEE Antennas Wireless Propagation Letters*, Vol. 19, No. 4, 591–595, 2020.
18. Sood, D. and C. C. Tripathi, "Broadband ultrathin low-profile metamaterial microwave absorber," *Appl. Phys. A*, Vol. 122, 332, 2016.
19. Singh, G., A. Sharma, and S. Ghosh, "A broadband multilayer circuit analog absorber using resistive ink," *Microwave Optical Technology Letters*, Vol. 63, 322–328, 2020.
20. Xiao, H., Z. Qu, M. Lv, H. Du, W, Zhu, C. Wang, and R. Qin, "Optically transparent broadband and polarization insensitive microwave metamaterial absorber," *Journal of Applied Physics*, Vol. 126, No. 13, 2019.
21. Ghosh, S., S. Bhattacharyya, and K. V. Srivastava, "Design, characterisation and fabrication of a broadband polarisation-insensitive multi-layer circuit analogue absorber," *IET Microwave Antennas Propagation*, Vol. 10, No. 8, 850–855, 2016.
22. Shang, Y., Z. Shen, and S. Xiao, "On the design of single-layer circuit analog absorber using double-square-loop array," *IEEE Transactions on Antennas and Propagation*, Vol. 61, No. 12, 6022–6029, Dec. 2013.
23. Tayde, Y., K. Chaudhary, G. Singh, et al., "An optically transparent and flexible microwave absorber for X and Ku bands application," *Microwave Optical Technology Letters*, Vol. 62, 1850–1859, 2020.
24. Li, F., P. Chen, Y. Poo, and R. Wu, "Achieving perfect absorption by the combination of dallenbach layer and salisbury screen," *Asia-Pacific Microwave Conference (APMC)*, 1507–1509, Kyoto, 2018.